PHYSICAL REVIEW D **92,** 114002 (2015)

$J/\psi(\eta_c)N$ and $\Upsilon(\eta_b)N$ cross sections

C. W. Xiao[1] and U.-G. Meißner[2,1]

[1]*Institut für Kernphysik (Theorie), Institute for Advanced Simulation, and Jülich Center for Hadron Physics, Forschungszentrum Jülich, D-52425 Jülich, Germany*

[2]*Helmholtz-Institut für Strahlen- und Kernphysik, and Bethe Center for Theoretical Physics, Universität Bonn, D-53115 Bonn, Germany*

(Received 11 August 2015; published 1 December 2015)

Inspired by the recent findings of the two P_c^+ states in the $J/\psi p$ mass spectrum at LHCb, we investigate the elastic and inelastic cross sections of the $J/\psi N$, $\eta_c N$, ΥN and $\eta_b N$ channels within the constraints from heavy quark spin and flavor symmetry. The $\bar{D}^{(*)}\Sigma_c^{(*)}$ ($B^{(*)}\Sigma_b^{(*)}$) bound states predicted in earlier works should be accessible in elastic and/or inelastic processes of the $J/\psi N$ and/or $\eta_c N$ (ΥN and/or $\eta_b N$) interactions.

DOI: 10.1103/PhysRevD.92.114002 PACS numbers: 12.38.Lg, 12.39.Hg, 13.85.Lg, 14.20.Pt

I. INTRODUCTION

Recently, the LHCb collaboration has reported the observation of two new P_c^+ states [1], $P_c(4380)^+$, ($\Gamma = 205$ MeV) (denoted as P_1) and $P_c(4450)^+$, ($\Gamma = 39$ MeV) (P_2), which are found in the $J/\psi p$ mass spectrum of the $\Lambda_b^0 \to J/\psi K^- p$ decays and consistent with pentaquark states. There are still some uncertainties in the LHCb analysis about the spin-parity J^P quantum numbers, with the possible assignments $(3/2^-, 5/2^+)$ respectively, or $(3/2^-, 5/2^+)$, $(5/2^+, 3/2^-)$. What is the nature of these two states? Soon after the experimental finding, they are considered as molecular states [2–5], but the molecular components are different among these works. Using the one-pion exchange model, Ref. [2] suggests that P_1 is a $\bar{D}^*\Sigma_c$ molecular state with ($I = 1/2$, $J = 3/2$) and P_2 $\bar{D}^*\Sigma_c^*$ state with ($I = 1/2$, $J = 5/2$). And, P_1 is also interpreted as a $\bar{D}^*\Sigma_c$ state with ($I = 1/2$, $J^P = 3/2^-$) but P_2 as a $\bar{D}^*\Lambda_c$ and $\bar{D}\Sigma_c^*$ mixture ($I = 1/2$, $J = 5/2^+$) within the QCD sum rule frame [3]. The work of Ref. [4] based on the chiral unitary approach claims the P_2 to be a mixed state made of $\bar{D}^*\Sigma_c$ and $\bar{D}^*\Sigma_c^*$ with $I = 1/2$, $J^P = 3/2^-$ by the analysis of the Λ_b decays [6,7]. Furthermore, with the formalism of an effective theory, Ref. [5] explains P_1 and P_2 as the molecular candidates of $\bar{D}\Sigma_c^*$ and $\bar{D}^*\Sigma_c$, respectively. But, Ref. [8] questions the explanation of the molecular state for these two new findings and suggest that they should be considered as multiquark configuration at the quark level. Following, these two states can be described as a five quark state of the diquark picture in the short range interaction at the quark level [9–11]. On the contrary, it is suggested that they could be just a kinematical effect (cusp effect) [12–14] generated from the triangle diagram singularity. Even though Refs. [12–14] conclude that the peaks are not real states but the singularity effect of the triangle diagram which leads to the cusp of the decay amplitudes, the authors of [12] comment with caution that the conclusion of the kinematical effect can be distinguished with the future experimental measurement of the $\chi_{c1}p$ mass distribution in the process of $\Lambda_b^0 \to K^-\chi_{c1}p$. Later, the $\chi_{c1}p$ component, making of the P_2 state, is investigated in the work of [15] utilizing the Weinberg compositeness condition [16] and an interesting analogy to the scalar meson $f_0(980)$ is drawn. Even if there are different opinions on the structure of these two new states, one should keep in mind that both of them are found in the $J/\psi p$ mass spectrum. This is the motivation of the present work to look into the $J/\psi N$ cross sections, where N represents the nucleon.

Due to the heavy quark masses of c, b, and the couplings not known in the heavy charm and beauty sectors, which lead to the symmetry breaking in the heavy sector, with some assumptions and extrapolations for the interaction Lagrangian, one can get some insight into the heavy charm and beauty baryons [17–21]. Working on the heavy sector, one should take into account the heavy quark spin and flavor symmetry [22–24], which has been applied to the heavy meson-meson interactions [25,26] and heavy meson-baryon interactions [27,28]. On the other hand, by assuming the SU(4) symmetry in charm sector, the works of [29–31] have predicted several narrow N^* and Λ^* states in the hidden charm and hidden beauty sectors. Furthermore, combining the heavy quark spin symmetry (HQSS) and the extended local hidden gauge formalism [32–34], Refs. [35,36] obtain consistent results with the former predictions in Refs. [29–31] but with extra predictions, summarized as a $\bar{D}\Sigma_c$ ($B\Sigma_b$) bound state with ($J = 1/2$, $I = 1/2$), a $\bar{D}\Sigma_c^*$ ($B\Sigma_b^*$) state with ($J = 3/2$, $I = 1/2$), a $I = 1/2$ $\bar{D}^*\Sigma_c$ ($B^*\Sigma_b$) state degenerate in ($J = 1/2$, $3/2$) and a $I = 1/2$ $\bar{D}^*\Sigma_c^*$ ($B^*\Sigma_b^*$) state degenerate in ($J = 1/2$, $3/2$, $5/2$), where the results of hidden beauty baryons are analogous to the ones in the hidden charm sector because of the heavy quark flavor symmetry. Based on these two works, we study the cross sections of the $J/\psi N$ and $\eta_c N$ (ΥN and $\eta_b N$) channels in the present work. In the next

section, our formalism is presented. Then, we show our results. Finally, we finish with the conclusions.

II. FORMALISM

Following the works of [35,36], we focus on the scattering amplitudes of the $J/\psi N$ and $\eta_c N$ (ΥN and $\eta_b N$) channels. The scattering amplitudes are evaluated by solving the coupled channels Bethe-Salpeter equation under the on shell factorization [37–39]

$$T = [1 - VG]^{-1} V, \tag{1}$$

where the propagator G is a diagonal matrix with the loop functions of a meson and a baryon, the element of which is given by

$$G_{ii}(s) = i \int \frac{d^4q}{(2\pi)^4} \frac{2M_i}{(P-q)^2 - M_i^2 + i\epsilon} \frac{1}{q^2 - m_i^2 + i\epsilon}, \tag{2}$$

where m_i, M_i are the masses of meson and baryon in ith channel, respectively, q is the four-momentum of the meson, and P is the total four-momentum of the meson and the baryon, thus, $s = P^2$. The kernel matrix V contains the interaction potentials which are derived from the Lagrangian. In the present work, following Refs. [35,36], we take the constraints from the HQSS into account, thus, the elements of V_{ij} for the ($J = 1/2$, $I = 1/2$) sector are given in Table I, and for the ($J = 3/2$, $I = 1/2$) sector in Table II, which are extrapolated to the hidden beauty sectors just by replacing the quark $\bar{c} \to \bar{b}$ for the corresponding mesons and $c \to b$ for the baryons. In Tables I and II, the coefficients μ_i^I, μ_{ij}^I ($i, j = 1, 2, 3$) and λ_2^I are the unknown low energy constants under the HQSS bases, which specify the isospin sector and can be related using $SU(3)$ flavor symmetry. Note that all

TABLE I. The elements V_{ij} corresponding to the channels in the $J = 1/2$, $I = 1/2$ sector.

$\eta_c N$	$J/\psi N$	$\bar{D}\Lambda_c$	$\bar{D}\Sigma_c$	$\bar{D}^*\Lambda_c$	$\bar{D}^*\Sigma_c$	$\bar{D}^*\Sigma_c^*$
μ_1	0	$\frac{\mu_{12}}{2}$	$\frac{\mu_{13}}{2}$	$\frac{\sqrt{3}\mu_{12}}{2}$	$-\frac{\mu_{13}}{2\sqrt{3}}$	$\sqrt{\frac{2}{3}}\mu_{13}$
	μ_1	$\frac{\sqrt{3}\mu_{12}}{2}$	$-\frac{\mu_{13}}{2\sqrt{3}}$	$-\frac{\mu_{12}}{2}$	$\frac{5\mu_{13}}{6}$	$\frac{\sqrt{2}\mu_{13}}{3}$
		μ_2	0	0	$\frac{\mu_{23}}{\sqrt{3}}$	$\sqrt{\frac{2}{3}}\mu_{23}$
			$\frac{1}{3}(2\lambda_2 + \mu_3)$	$\frac{\mu_{23}}{\sqrt{3}}$	$\frac{2(\lambda_2 - \mu_3)}{3\sqrt{3}}$	$\frac{1}{3}\sqrt{\frac{2}{3}}(\mu_3 - \lambda_2)$
				μ_2	$-\frac{2\mu_{23}}{3}$	$\frac{\sqrt{2}\mu_{23}}{3}$
					$\frac{1}{9}(2\lambda_2 + 7\mu_3)$	$\frac{1}{9}\sqrt{2}(\mu_3 - \lambda_2)$
						$\frac{1}{9}(\lambda_2 + 8\mu_3)$

TABLE II. The elements V_{ij} corresponding to the channels in the $J = 3/2$, $I = 1/2$ sector.

$J/\psi N$	$\bar{D}^*\Lambda_c$	$\bar{D}^*\Sigma_c$	$\bar{D}\Sigma_c^*$	$\bar{D}^*\Sigma_c^*$
μ_1	μ_{12}	$\frac{\mu_{13}}{3}$	$-\frac{\mu_{13}}{\sqrt{3}}$	$\frac{\sqrt{5}\mu_{13}}{3}$
	μ_2	$\frac{\mu_{23}}{3}$	$-\frac{\mu_{23}}{\sqrt{3}}$	$\frac{\sqrt{5}\mu_{23}}{3}$
		$\frac{1}{9}(8\lambda_2 + \mu_3)$	$\frac{\lambda_2 - \mu_3}{3\sqrt{3}}$	$\frac{1}{9}\sqrt{5}(\mu_3 - \lambda_2)$
			$\frac{1}{3}(2\lambda_2 + \mu_3)$	$\frac{1}{3}\sqrt{\frac{5}{3}}(\lambda_2 - \mu_3)$
				$\frac{1}{9}(4\lambda_2 + 5\mu_3)$

of them just depend on the isospin (I) sector and are independent of the spin J, which is a consequence of the HQSS constraints. The values of the coefficients are dependent on the model used. As discussed in the introduction, using the local hidden gauge formalism, we obtain their values for the two spin sectors

$$\begin{aligned}
\mu_2 &= \frac{1}{4f_\pi^2}(k^0 + k'^0), \\
\mu_3 &= -\frac{1}{4f_\pi^2}(k^0 + k'^0), \\
\mu_{12} &= -\sqrt{6}\frac{m_\rho^2}{p_{D^*}^2 - m_{D^*}^2}\frac{1}{4f_\pi^2}(k^0 + k'^0), \\
\mu_1 &= 0, \qquad \mu_{23} = 0, \\
\lambda_2 &= \mu_3, \qquad \mu_{13} = -\mu_{12},
\end{aligned} \tag{3}$$

where p_{D^*} and m_{D^*} are the four momentum and the mass of D^* (for the hidden beauty cases just changing to the ones of B^*), f_π the pion decay constant, and k^0, k'^0 are the energies of the incoming and outgoing mesons (for the vector mesons, we have ignored the factor $\vec{\epsilon}\vec{\epsilon}'$).[1] Of course, these are only the leading/lowest order (LO) interactions and eventually higher order terms need to be taken into account. For a first estimate has given here, such an approach is, however, justified. For example, in the $\bar{K}N$ interaction, the results of LO are well explained the experimental data [38,39] and lie inside the uncertainty bands of the higher order calculations [43]. In principle, one should perform higher order calculations. However, to deal with the parameters appearing at next to leading order (NLO) as done in e.g. Ref. [43], one needs a certain amount of data which for the channels one considers. Such data do not yet exist for our present cases. See also Ref. [21] which tries to

[1]Indeed, this factor will lead to a correction coefficient in the G-function of $\vec{q}^2/(3M_V^2)$ as shown in Ref. [40], which is negligibly small in the threshold region [41,42]. Thus, it factorizes also in the T matrix for the external vector mesons, and is therefore ignored. This approximation needs, however, to be scrutinized in more detail in future works.

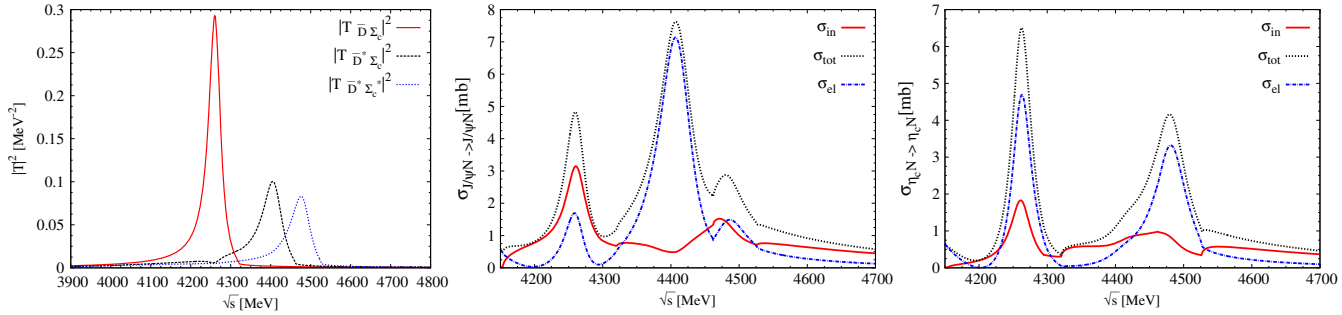

FIG. 1 (color online). Results of the $J = 1/2$, $I = 1/2$ sector with hidden charm. Left: Modulus squared of the amplitudes. Middle: The total (dash/black line), elastic (dot-dash/blue line) and inelastic (solid/red line) cross sections of the $J/\psi N$ channel. Right: The total, elastic and inelastic cross sections for the $\eta_c N$ channel.

extend calculations from LO to NLO following the method of Ref. [44] and faces the lack of enough experimental information to control the free parameters at NLO. We consider our calculation as a first estimate that needs to be refined and sharpened in the future.

In the present work, we investigate the $J/\psi N$ and $\eta_c N$ (ΥN and $\eta_b N$) channels by evaluating their cross sections. Using the optical theorem, we obtain

$$\sigma_{\rm tot} = -\frac{M_N}{P_{cm}^{J/\psi}\sqrt{s}}{\rm Im}T_{J/\psi N\to J/\psi N}, \tag{4}$$

where $P_{cm}^{J/\psi}$ is the momentum of J/ψ in the center mass frame and M_N the mass of nucleon, and one defines the elastic cross section

$$\sigma_{\rm el} = \frac{1}{4\pi}\frac{M_N^2}{s}\overline{\sum}\sum|T_{J/\psi N\to J/\psi N}|^2, \tag{5}$$

where $\sum$, $\overline{\sum}$ stand for sum and average over the spins of the nucleons and J/ψ. Hence, the inelastic cross section is given by

$$\begin{aligned}\sigma_{\rm in} &= \sigma_{\rm tot} - \sigma_{\rm el}\\ &= -\frac{M_N}{P_{cm}^{J/\psi}\sqrt{s}}{\rm Im}T_{J/\psi N\to J/\psi N}\\ &\quad -\frac{1}{4\pi}\frac{M_N^2}{s}\overline{\sum}\sum|T_{J/\psi N\to J/\psi N}|^2.\end{aligned} \tag{6}$$

We remark that measurements of elastic and inelastic cross sections depend on the energy of the initial beams (up to the inelastic threshold or not) and the specific processes related (what products in the final states). In the low energy region, hadron scattering is elastic, and then up to some threshold, other channel(s) open and the inelastic scattering contributes to the cross sections. For example, the $\pi\pi$ scattering amplitude is dominantly elastic scattering up to about 1 GeV, the first inelasticity starting at the 4π, which is, however, very weak. The first noticeable inelasticity actually sets in at the $K\bar{K}$. Both these channels contribute to the inelastic $\pi\pi$ scattering amplitude. In our formalism, we use a coupled channel approach to evaluate the scattering amplitude, where the coupled channels are assumed as intermediate states (not the final states), and thus, for a specified channel, the scattering is elastic or not referring to whether the coupled channels open in the final states. Therefore, for our predicted bound states, they could be found in the elastic scattering of some channels. For the present cases, the $J/\psi N$ and $\eta_c N$ (ΥN and $\eta_b N$) interactions are elastic or inelastic also depending on the energy of the initial beams and the experimental measurements of the final states, which we are, however, not concerned about here.

III. RESULTS AND DISCUSSIONS

Using the coupled channel approach, all the channels that we are concerned with can be seen in Tables I and II, are $\eta_c N$, $J/\psi N$, $\bar{D}\Lambda_c$, $\bar{D}\Sigma_c$, $\bar{D}^*\Lambda_c$, $\bar{D}^*\Sigma_c$, $\bar{D}\Sigma_c^*$, $\bar{D}^*\Sigma_c^*$ for the hidden charm sector ($J = 1/2, 3/2$), and $\eta_b N$, ΥN, $B\Lambda_b$, $B\Sigma_b$, $B^*\Lambda_b$, $B^*\Sigma_b$, $B\Sigma_b^*$, $B^*\Sigma_b^*$ for the hidden beauty sector ($J = 1/2, 3/2$). Then, with Eqs. (1), (4), (5) and (6), we can evaluate the scattering amplitudes and the cross sections. We show our result of hidden charm in the $J = 1/2$, $I = 1/2$ sector in Fig. 1. In the left of Fig. 1, we have reproduced the results of [35], where the three predicted bound states are clearly seen in the squares of the scattering amplitudes for the channels $\bar{D}\Sigma_c$, $\bar{D}^*\Sigma_c$, $\bar{D}^*\Sigma_c^*$ respectively, with the masses 4262 MeV, 4410 MeV, 4481 MeV and the widths 35 MeV, 58 MeV, 57 MeV respectively. These three states are also seen in the total and elastic cross sections of the $J/\psi N$ channel, seen in the middle of Fig. 1. Interestingly, the second state of $\bar{D}^*\Sigma_c$ cannot be found in the inelastic cross section,[2] which means that this state

[2]Since this state couples strongly to the $J/\psi N$ channel [35], the strong coupled effects enhance the scattering amplitude in the energy region of this peak/pole and thus lead to the big elastic cross section. Even though the transition of $\bar{D}^*\Sigma_c \to J/\psi N$ is suppressed in the local hidden gauge formalism, its coupled channel effects are allowed under the heavy quark spin symmetry constraints with a positive factor $\frac{5}{6}$, as seen in Table I, which leads to a constructive interference and the strong coupling.

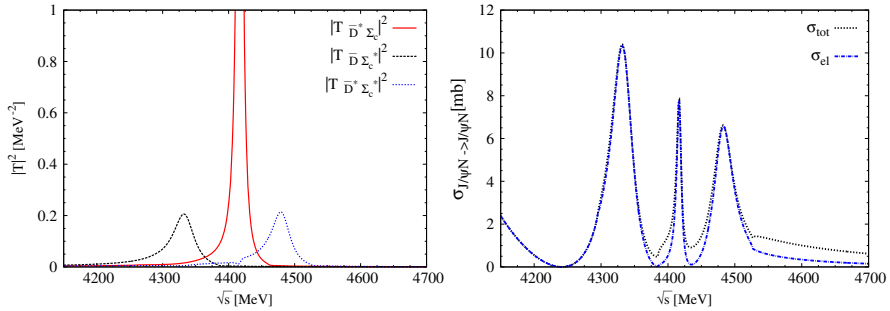

FIG. 2 (color online). Result of the $J = 3/2$, $I = 1/2$ sector with hidden charm. Left: Modulus squared of the amplitudes. Right: The total (dash/black line) and elastic (dot-dash/blue line) cross sections of the $J/\psi N$ channel.

would not be seen in the inelastic process and coincides with the fact of the experimental finding for only two P_c^+ states found in the $J/\psi p$ mass spectrum in Ref. [1]. Note that our results do not take into account any background and the theoretical uncertainties. Even though we find three states in the two-body scattering, when we look into the inelastic scattering cross section, only two of them can be found. The results of Ref. [45] reveal that the peak seen in the inelastic cross section would be destroyed by the Fermi motion of the nuclear target. But, these peaks can also be looked for in other inelastic processes, like decay model of Ref. [1], where the $J/\psi p$ final state interaction is inelastic since there is another product of K^- in the decay process. Thus, we suggest that our predicted states, $\bar{D}\Sigma_c$ and $\bar{D}^*\Sigma_c^*$, could be looked for in other inelastic processes of the $J/\psi N$ final state. When we look at the cross sections of the $\eta_c N$ channel in the right of Fig. 1, the state of $\bar{D}^*\Sigma_c$ is still missing in the total and elastic cross sections since it couples to $\eta_c N$ channel weakly [35], and the state of $\bar{D}^*\Sigma_c^*$ disappears in the inelastic cross section. In fact, the transition of $\bar{D}^*\Sigma_c \to \eta_c N$ is doubly suppressed due to the heavy D meson exchange and the weak Yukawa coupling in the $DN\Sigma_c$ vertex in the local hidden gauge formalism. On the other hand, under the heavy quark spin symmetry constraints, the $\eta_c N$ channel couples to $\bar{D}^*\Sigma_c$ channel with a negative factor $-\frac{1}{2\sqrt{3}}$, as seen in Table I, which leads to the destructive interference effects and the weak coupling for two channels. This leads to the $\bar{D}^*\Sigma_c$ state mixing in the $\eta_c N$ channel. To summarize, we find that only one of the $\bar{D}\Sigma_c$ is found in both the inelastic scattering of the $J/\psi N$ and $\eta_c N$[3] final state interaction, the second one just can be seen in the elastic scattering of the $J/\psi N$ interaction, and the one of $\bar{D}^*\Sigma_c^*$ can be looked for in the inelastic scattering of the $J/\psi N$ interaction and elastic scattering of the $\eta_c N$ channel.

The results of hidden charm in the $J = 3/2$, $I = 1/2$ sector are shown in Fig. 2. The three predicted states [35] are seen in the clear peaks of the modulus squared of the amplitudes in the left panel of Fig. 2, which are a bit below the thresholds of $\bar{D}\Sigma_c^*$, $\bar{D}^*\Sigma_c$, $\bar{D}^*\Sigma_c^*$ channels, respectively, with the masses 4334 MeV, 4417 MeV, 4481 MeV and the widths 38 MeV, 8 MeV, 35 MeV respectively. The structures of the three peaks corresponding to these states are also seen in the total and elastic cross sections of the $J/\psi N$ channel in the right panel of Fig. 2, where we find that the total cross section is essentially given by the elastic one. Therefore, these three states could only be found in the elastic processes of the $J/\psi N$ interaction.

With the heavy quark flavor symmetry and using similar dynamics of the interaction potentials, we extrapolate our formalism into the hidden beauty sector. Our results are shown in Figs. 3 and 4 for the sectors of $J = 1/2$, $I = 1/2$ and $J = 3/2$, $I = 1/2$ respectively. In the left panel of Fig. 3, the predicted states of Ref. [36] have been reproduced in the scattering amplitudes of the $B\Sigma_b$, $B^*\Sigma_b$, $B^*\Sigma_b^*$ channels, respectively, where the masses of these three peaks are 10961 MeV, 11002 MeV, 11023 MeV and the widths are 12 MeV, 26 MeV, 28 MeV, respectively. All of them appear as resonant structures in the total and elastic cross sections of the ΥN channel in the middle panel of Fig. 3, where the peak for the third state is nearly washed out. We also find that the second peak is enhanced since it couples to ΥN channel strongly [36], which leads to an elastic cross section larger than the total one determined by Eq. (4). Therefore, in the inelastic cross sections, analogous to the hidden charm sector, the second one disappears and only the other two keep showing up. For the cross sections of the $\eta_b N$ channel, shown in the right panel of Fig. 3, like the results for hidden charm, only the first one and the third one show up in the total and elastic cross sections since the second one of the $B^*\Sigma_b$ couples to the $\eta_b N$ channel weakly [36], and only the first one survives in the inelastic cross sections. Thus, we can see that the $B\Sigma_b$ bound state can be found in both of the ΥN and $\eta_b N$ final state interactions with elastic and inelastic processes. The second one of $B^*\Sigma_b$ only can be seen in the ΥN elastic process. And the state of $B^*\Sigma_b^*$ can be found both elastic and inelastic process of the ΥN interaction, and in the elastic process of the $\eta_b N$ channel.

In the left panel of Fig. 4, one finds three peaks below the thresholds of $B\Sigma_b^*$, $B^*\Sigma_b$, $B^*\Sigma_b^*$, respectively, with the

[3]The $\eta_c p$ channel is dominant for the decay of the low-lying $1/2^-$ state as claimed in Refs. [11,46].

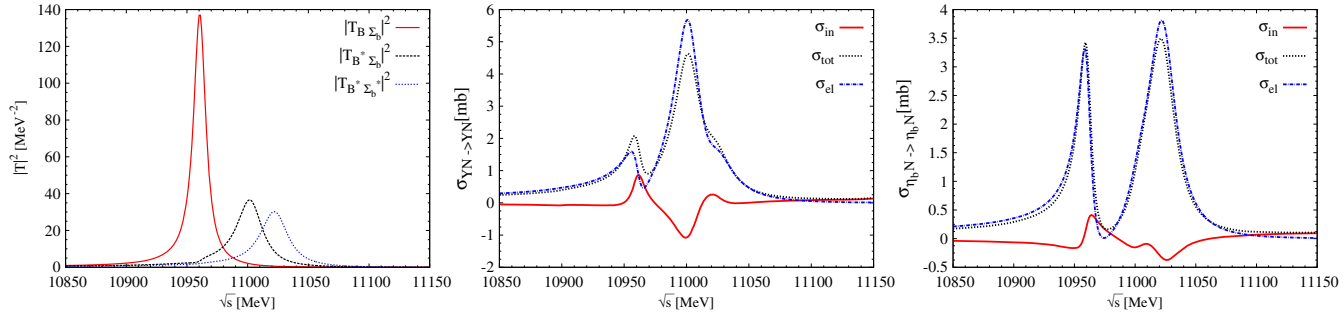

FIG. 3 (color online). Result of the $J = 1/2$, $I = 1/2$ sector with hidden beauty. Left: Modulus squared of the amplitudes. Middle: The total, elastic and inelastic cross sections of the ΥN channel. Right: The total, elastic and inelastic cross sections for the $\eta_b N$ channel. (Analogous to Fig. 1).

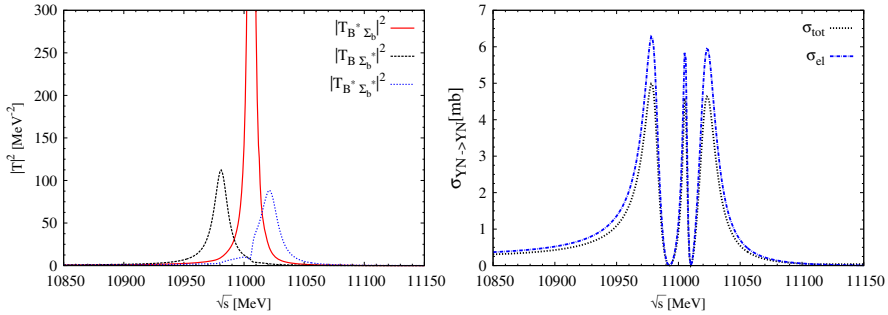

FIG. 4 (color online). Result of the $J = 3/2$, $I = 1/2$ sector with hidden beauty. Left: Modulus squared of the amplitudes. Right: The total, elastic and inelastic cross sections of the ΥN channel. (Analogous to Fig. 2).

masses 10981 MeV, 11006 MeV, 11022 MeV and the widths about 14 MeV, 4 MeV, 17 MeV accordingly, which are consistent with Ref. [36]. These structures of the resonant peak are also found in the total and elastic cross sections, shown in the right panel of Fig. 4, but surprisingly the total cross section determined by the optical theorem, Eq. (4), is smaller than the elastic one because of the large momentum transfer in the ΥN channel which reduces the total cross section. Therefore, the three predicted states in Ref. [36] can be seen in the elastic ΥN final interactions.

Due the lack of the experimental data to determine the free parameters, as discussed before, the results above are obtained with these parameters in range of their natural values, that is ($a(\mu) \sim -2$ and $\mu \simeq q_{\rm max} \sim 1000$ MeV) [39]. We take $a(\mu) = -2.3$ with $\mu = 1000$ MeV for the loop function of the dimensional regularization as done in Refs. [29,30] for the hidden charm sector, which is equivalent to taking $q_{\rm max} = 820$ MeV with the cutoff method for the loop function as discussed in Ref. [35], and take $q_{\rm max} = 2000$ MeV for the hidden beauty sector since we have introduced a form factor in the loop functions for the higher momentum transfer in the hidden beauty sector, which is different from Ref. [31] (more details seen Ref. [36]). To estimate the uncertainties, one can make 10% changes to the parameters $a(\mu)$ or $q_{\rm max}$, which are still in their natural ranges, and keeping $\mu = 1000$ MeV unchanged for the dimension regularization method since its changes can be compensated by adjusting $a(\mu)$ [39]. We

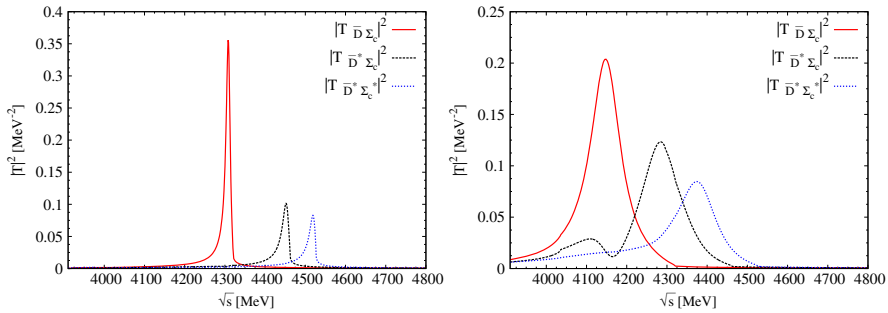

FIG. 5 (color online). Uncertainties for the $J = 1/2$, $I = 1/2$ sector with hidden charm. Left: Parameter reduces 10%. Right: Parameter increases 10%.

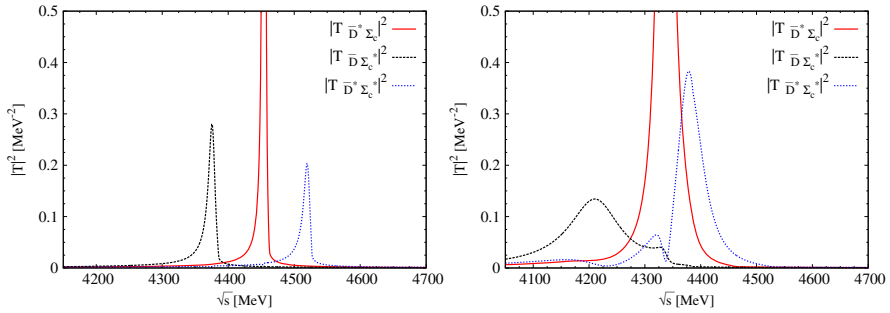

FIG. 6 (color online). Uncertainties for the $J = 3/2$, $I = 1/2$ sector with hidden charm. (Analogous to Fig. 5).

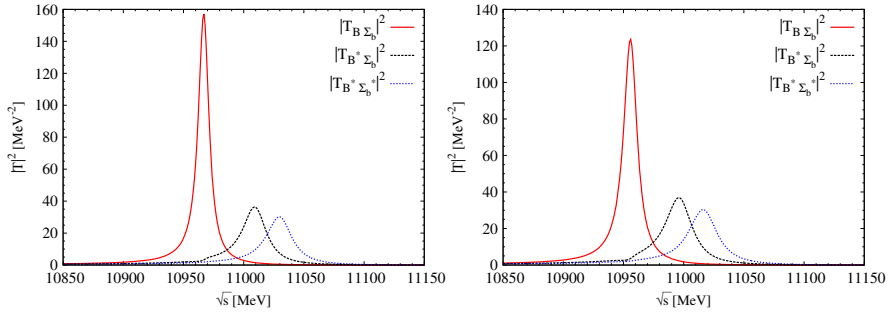

FIG. 7 (color online). Uncertainties for the $J = 1/2$, $I = 1/2$ sector with hidden beauty. (Analogous to Fig. 5).

show our results in Figs. 5–8 for both the hidden charm and the hidden beauty sectors with spin $J = \frac{1}{2}$ and $J = \frac{3}{2}$ when the parameters change $\pm 10\%$. Compared Fig. 5 with Fig. 1 (Left), we can see that the peaks move to higher energies when the parameter reduces 10%, and the peaks move to lower energies while the parameter increases 10%. The others are similar when the parameters change. For the peaks in Fig. 5, we search for the poles in the second Riemann sheet, obtained (mass, width) as (4309, 13) MeV, (4455, 21) MeV, (4522, 20) MeV (Left), and (4144, 91) MeV, (4290, 124) MeV, (4382, 124) (Right), for the channels $\bar{D}\Sigma_c$, $\bar{D}^*\Sigma_c$, $\bar{D}^*\Sigma_c^*$ respectively. For the peaks in Fig. 6, we obtain (4377, 12) MeV, (4454, 3) MeV, (4521, 12) MeV (Left), and (4202, 104) MeV, (4336, 23) MeV, (4379, 53) MeV (Right), for the channels $\bar{D}\Sigma_c^*$, $\bar{D}^*\Sigma_c$, $\bar{D}^*\Sigma_c^*$ respectively. In Fig. 7, we find the poles as (10967, 11) MeV, (11010, 24) MeV, (11030, 26) MeV (Left), and (10956, 14) MeV, (10997, 27) MeV, (11017, 29) MeV (Left), for the channels $B\Sigma_b$, $B\Sigma_b^*$, $B^*\Sigma_b^*$ respectively. In Fig. 8, we search the corresponded poles as (10987, 12) MeV, (11012, 4) MeV, (11029,17) (Left), and (10976, 16) MeV, (11002, 5) MeV, (11016, 17) MeV (Right), for the channels $B\Sigma_b^*$, $B^*\Sigma_b$, $B^*\Sigma_b^*$ respectively. Because of introducing the form factor in the loop functions in the hidden beauty sector, we can see that the results are more stable than the ones in the hidden charm sector as discussed in Ref. [36], which are consistent with the results obtained in Ref. [31]. Therefore, the uncertainties in the hidden beauty sector are much smaller than the ones of the hidden charm sector. Furthermore, from the strengths of the modulus squared of the scattering amplitudes in Figs. 5–8, one can

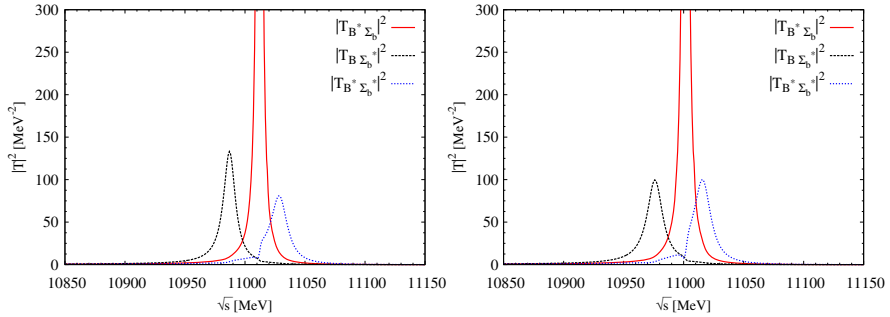

FIG. 8 (color online). Uncertainties for the $J = 3/2$, $I = 1/2$ sector with hidden beauty. (Analogous to Fig. 5).

TABLE III. Our results for the predicted states with uncertainties (units: MeV).

Channels (states)	Thresholds	$J^P=\frac{1}{2}^-$ (mass, width)	$J^P=\frac{3}{2}^-$ (mass, width)	Experiments
$\bar{D}\Sigma_c$	4320.8	$(4262^{+47}_{-118}, 35^{-22}_{+56})$	.....	...
$\bar{D}\Sigma_c^*$	4385.3	.....	$(4334^{+43}_{-132}, 38^{-26}_{+66})$	$P_c(4380)^+$?
$\bar{D}^*\Sigma_c$	4462.2	$(4410^{+45}_{-120}, 58^{-37}_{+66})$	$(4417^{+37}_{-81}, 8^{-5}_{+15})$	$P_c(4450)^+$?
$\bar{D}^*\Sigma_c^*$	4526.7	$(4481^{+41}_{-99}, 57^{-37}_{+67})$	$(4481^{+40}_{-102}, 35^{-23}_{+18})$	$P_c(4450)^+$?
$B\Sigma_b$	11092.8	$(10961^{+6}_{-5}, 12^{-1}_{+2})$	.....	...
$B\Sigma_b^*$	11113.0	.....	$(10981^{+6}_{-5}, 14^{-2}_{+2})$	...
$B^*\Sigma_b$	11138.6	$(11002^{+8}_{-5}, 26^{-2}_{+1})$	$(11006^{+6}_{-4}, 4^{-0}_{+1})$	...
$B^*\Sigma_b^*$	11158.8	$(11023^{+7}_{-6}, 28^{-2}_{+1})$	$(11022^{+7}_{-6}, 17^{-0}_{+0})$	...

estimate the uncertainties of 10% to 40% differences for the cross sections. Finally, we summarize our results in Table III, where the errors of the masses and widths are anticorrelated since the states become less bound (masses increase) and thus the further away decay channels lead to reduced widths. From that table, we can see that the mass of the predicted $\bar{D}\Sigma_c^*$ bound state is close to the $P_c(4380)^+$ with the uncertainties, and its quantum number $J^P=\frac{3}{2}^-$ is consistent with one of the experimental assignments, but its width is much smaller than the experimental measurement for the $P_c(4380)^+$ even though one takes into account the maximum of uncertainties (maybe there are more other decay channels as suggested in Ref. [47]). Or, this predicted $\bar{D}\Sigma_c^*$ state is just a spin partner of the $P_c(4380)^+$ state which is analogous to the $X(3872)$ and $Z_b(10610)/Z_b'(10650)$ [26]. Within the uncertainties, the masses and the widths of the $\bar{D}^*\Sigma_c$ and $\bar{D}^*\Sigma_c^*$ bound states are consistent with the experiment findings for the $P_c(4450)^+$, and its $J^P=\frac{3}{2}^-$ is also one of the experimental assignments. Thus, the $P_c(4450)^+$ state could be a molecule of the $\bar{D}^*\Sigma_c$ or the $\bar{D}^*\Sigma_c^*$, or a mixture of two of them as claimed in Ref. [4]. Note that, since the two P_c states are of opposite parity, only one of them with the minus parity can be associated with our results. These are also some uncertainties for the structure and the spin assignments of the two P_c states in LHCb findings, and thus, this is why we investigate the elastic and inelastic cross sections in the present work which need the further experiments to confirm our conclusions. On the other hand, there are other predictions under the heavy quark spin and flavor symmetries in Table III (Ref. [11] also predicts several resonances around 4040–4500 MeV with $J^P=1/2^-, 3/2^-$) which also require future experiments to look for our predictions.[4]

[4]One should keep in mind that the ignored factor of $\vec{\varepsilon}\vec{\varepsilon}'$, which is spin-independent, leads to some states degenerate in spin, $1/2^-$, $3/2^-$, $5/2^-$, as concluded in Refs. [35,36].

Furthermore, the uncertainties coming from the symmetry breaking effects should be stressed. As mentioned in the introduction, for the heavy quark masses of the charm and beauty, the SU(4) and SU(5) symmetries are badly broken at the quark level. However, how strongly these breaking effects are reflected on the hadronic level are not well established because the couplings in the heavy sectors are not known. Taking the coupling of $g_{DD\rho}$ for example, under the SU(4) symmetry one can obtain the value of $g_{DD\rho}=g_{KK\rho}=g_{\pi\pi\rho}/2\simeq 3$ [48–50], compared to the others, $g_{DD\rho}\simeq 5$ with the framework of the Dyson-Schwinger equation [51], $g_{DD\rho}\simeq 4.8$ in the $2+1$ flavor lattice QCD [52], $g_{DD\rho}\simeq 3.8$ with the light-cone QCD sum rules [53], $g_{DD\rho}\simeq 2.9$ or 4.3 with the three-point QCD sum rule [54], $g_{DD\rho}\simeq 2.6$ with the light-cone QCD sum rules [55]. Therefore, there are also some uncertainties about the symmetry breaking effects in different models. Theoretically, on one hand, ignored the breaking effects and then under the symmetry constraints, Ref. [48] predicts some possible bound states in the related strangeness, charm and beauty two-body systems which is analogous to the $K\bar{K}$ system, and the work of [49] find that the properties of the $\bar{D}N$ interaction are similar to the KN interaction. In this assumption, in fact, the SU(4) or SU(5) symmetry is equivalently reduced to the SU(3) symmetry framework by just replacing the s quark with the c or b quark if the systems are not combined with themselves (s, c, b). On the other hand, one can take into account the symmetry breaking effects by specifying the related decay constants for the potentials of the different channels which are derived from the Lagrangian, for example the factor of the decay constants $1/f^2$ [Eq. (3) taking $f=f_\pi$] is replaced by $1/f_{D^*}^2$ for the hidden charm sector as done in Ref. [56]. Alternatively, if we have enough experimental data to determine the parameters, the symmetry breaking effects can be absorbed into the free $1/f^2$ [38]. Or we can roughly estimate the effects as done in Ref. [35] by adding a factor to the potentials for the $1/f^2$. To summarize, there are also some uncertainties when we consider the symmetry breaking but

these are difficult to specify quantitatively (more discussions can be referred to Refs. [35,56]).

IV. CONCLUSIONS

We have investigated the elastic and inelastic cross sections of the $J/\psi N$, $\eta_c N$, ΥN and $\eta_b N$ channels using an extended local hidden gauge formalism supplemented with constraints from heavy quark spin and flavor symmetry. The predicted bound states in the earlier works of Refs. [35,36], $\bar{D}\Sigma_c$, $\bar{D}^*\Sigma_c$, $\bar{D}\Sigma_c^*$, $\bar{D}^*\Sigma_c^*$ and $B\Sigma_b$, $B^*\Sigma_b$, $B\Sigma_b^*$, $B^*\Sigma_b^*$ with spin $J = 1/2, 3/2$, should appear in elastic and/or inelastic final-state interactions of the $J/\psi N$, $\eta_c N$ and ΥN, $\eta_b N$ channels, respectively. Clearly, these are only rough estimates due to the various approximations entering the formalism used. Note also that the hidden beauty states have already been discussed in Refs. [2,57]. Furthermore, since we work in the isospin bases, for experimental searches it is advisable to look for the predicted states with isospin $I = 1/2$ in the $J/\psi p/n$, $\eta_c p/n$, $\Upsilon p/n$ and $\eta_b p/n$ (p/n are the proton and neutron) elastic or inelastic interaction processes in the future, where the predicted neutral partners P_c^0 [10] of the P_c^+ states [1] may be found in these processes.

ACKNOWLEDGMENTS

We thank C. Hanhart, Q. Wang, J. A. Oller and J. Nieves for useful discussions, and are grateful to E. Oset and F. K. Guo for useful comments and a careful reading the manuscript. This work is supported in part by the DFG and the NSFC through funds provided to the Sino-German CRC 110 "Symmetries and the Emergence of Structure in QCD". This work is also supported in part by The Chinese Academy of Sciences CAS President's International Fellowship Initiative (PIFI) Grant No. 2015VMA076.

Note added.—Soon after this work, Ref. [58] also predicts a $B^*\Sigma_b$ state P_b, which can be looked for in the Υp channel.

[1] R. Aaij *et al.* (LHCb Collaboration), Observation of $J/\psi p$ Resonances Consistent with Pentaquark States in $\Lambda_b^0 \to J/\psi K^- p$ Decays, Phys. Rev. Lett. **115**, 072001 (2015).
[2] R. Chen, X. Liu, X. Q. Li, and S. L. Zhu, A New Page for Hadron Physics: Identifying Exotic Hidden-Charm Pentaquarks, Phys. Rev. Lett. **115**, 132002 (2015).
[3] H. X. Chen, W. Chen, X. Liu, T. G. Steele, and S. L. Zhu, Towards Exotic Hidden-Charm Pentaquarks in QCD, Phys. Rev. Lett. **115**, 172001 (2015).
[4] L. Roca, J. Nieves, and E. Oset, The LHCb pentaquark as a $\bar{D}^*\Sigma_c - \bar{D}^*\Sigma_c^*$ molecular state, Phys. Rev. D **92**, 094003 (2015).
[5] J. He, The $\bar{D}^*\Sigma_c^*$ and $\bar{D}^*\Sigma_c$ interactions and the LHCb hidden-charmed pentaquarks, arXiv:1507.05200.
[6] L. Roca, M. Mai, E. Oset, and U.-G. Meißner, Predictions for the $\Lambda_b \to J/\psi\Lambda(1405)$ decay, Eur. Phys. J. C **75**, 218 (2015).
[7] A. Feijoo, V. K. Magas, A. Ramos, and E. Oset, The $\Lambda_b \to J/\psi K\Xi$ decay and the higher order chiral terms of the meson baryon interaction, Phys. Rev. D **92**, 076015 (2015).
[8] A. Mironov and A. Morozov, Is pentaquark doublet a hadronic molecule?, arXiv:1507.04694.
[9] L. Maiani, A. D. Polosa, and V. Riquer, The new pentaquarks in the diquark model, Phys. Lett. B **749**, 289 (2015).
[10] R. F. Lebed, The pentaquark candidates in the dynamical diquark picture, Phys. Lett. B **749**, 454 (2015).
[11] V. V. Anisovich, M. A. Matveev, J. Nyiri, A. V. Sarantsev, and A. N. Semenova, Pentaquarks and resonances in the pJ/ψ spectrum, arXiv:1507.07652.
[12] F. K. Guo, U.-G. Meißner, W. Wang, and Z. Yang, How to reveal the exotic nature of the $P_c(4450)$, Phys. Rev. D **92**, 071502 (2015).
[13] X. H. Liu, Q. Wang, and Q. Zhao, Understanding the newly observed heavy pentaquark candidates, arXiv:1507.05359.
[14] M. Mikhasenko, A triangle singularity and the LHCb pentaquarks, arXiv:1507.06552.
[15] U.-G. Meißner and J. A. Oller, Testing the $\chi_{c1} p$ composite nature of the $P_c(4450)$, Phys. Lett. B **751**, 59 (2015).
[16] S. Weinberg, Evidence that the deuteron is not an elementary particle, Phys. Rev. **137**, B672 (1965).
[17] T. Mizutani and A. Ramos, D mesons in nuclear matter: A DN coupled-channel equations approach, Phys. Rev. C **74**, 065201 (2006).
[18] J. Haidenbauer, G. Krein, U.-G. Meißner, and L. Tolos, DN interaction from meson exchange, Eur. Phys. J. A **47**, 18 (2011).
[19] J. He, Z. Ouyang, X. Liu, and X. Q. Li, Production of charmed baryon $\Lambda_c(2940)^+$ at PANDA, Phys. Rev. D **84**, 114010 (2011).
[20] Z. C. Yang, Z. F. Sun, J. He, X. Liu, and S. L. Zhu, The possible hidden-charm molecular baryons composed of anti-charmed meson and charmed baryon, Chin. Phys. C **36**, 6 (2012).
[21] J. X. Lu, Y. Zhou, H. X. Chen, J. J. Xie, and L. S. Geng, Dynamically generated $J^P = 1/2^-(3/2^-)$ singly charmed and bottom heavy baryons, Phys. Rev. D **92**, 014036 (2015).
[22] N. Isgur and M. B. Wise, Weak decays of heavy mesons in the static quark approximation, Phys. Lett. B **232**, 113 (1989).
[23] M. Neubert, Heavy quark symmetry, Phys. Rep. **245**, 259 (1994).

[24] A. V. Manohar and M. B. Wise, *Heavy Quark Physics*, Cambridge Monographs on Particle Physics, Nuclear Physics and Cosmology, Vol. 10 (Cambridge University Press, Cambridge, England, 2000).

[25] F. K. Guo, C. Hanhart, and U.-G. Meißner, Implications of Heavy Quark Spin Symmetry on Heavy Meson Hadronic Molecules, Phys. Rev. Lett. **102**, 242004 (2009).

[26] F. K. Guo, C. Hidalgo-Duque, J. Nieves, and M. P. Valderrama, Consequences of heavy quark symmetries for hadronic molecules, Phys. Rev. D **88**, 054007 (2013).

[27] C. Garcia-Recio, V. K. Magas, T. Mizutani, J. Nieves, A. Ramos, L. L. Salcedo, and L. Tolos, The s-wave charmed baryon resonances from a coupled-channel approach with heavy quark symmetry, Phys. Rev. D **79**, 054004 (2009).

[28] D. Gamermann, C. Garcia-Recio, J. Nieves, L. L. Salcedo, and L. Tolos, Exotic dynamically generated baryons with negative charm quantum number, Phys. Rev. D **81**, 094016 (2010).

[29] J. J. Wu, R. Molina, E. Oset, and B. S. Zou, Prediction of Narrow N^* and Λ^* Resonances with Hidden Charm above 4 GeV, Phys. Rev. Lett. **105**, 232001 (2010).

[30] J. J. Wu, R. Molina, E. Oset, and B. S. Zou, Dynamically generated N^* and Λ^* resonances in the hidden charm sector around 4.3 GeV, Phys. Rev. C **84**, 015202 (2011).

[31] J. J. Wu and B. S. Zou, Prediction of super-heavy N^* and Λ^* resonances with hidden beauty, Phys. Lett. B **709**, 70 (2012).

[32] M. Bando, T. Kugo, and K. Yamawaki, Nonlinear realization and hidden local symmetries, Phys. Rep. **164**, 217 (1988).

[33] U.-G. Meißner, Low-energy hadron physics from effective chiral Lagrangians with vector mesons, Phys. Rep. **161**, 213 (1988).

[34] M. Harada and K. Yamawaki, Hidden local symmetry at loop: A New perspective of composite gauge boson and chiral phase transition, Phys. Rep. **381**, 1 (2003).

[35] C. W. Xiao, J. Nieves, and E. Oset, Combining heavy quark spin and local hidden gauge symmetries in the dynamical generation of hidden charm baryons, Phys. Rev. D **88**, 056012 (2013).

[36] C. W. Xiao and E. Oset, Hidden beauty baryon states in the local hidden gauge approach with heavy quark spin symmetry, Eur. Phys. J. A **49**, 139 (2013).

[37] J. A. Oller and E. Oset, Chiral symmetry amplitudes in the S wave isoscalar and isovector channels and the sigma, f0 (980), a0(980) scalar mesons, Nucl. Phys. **A620**, 438 (1997); Nucl. Phys. **A652**, 407(E) (1999).

[38] E. Oset and A. Ramos, Nonperturbative chiral approach to s wave anti-K N interactions, Nucl. Phys. **A635**, 99 (1998).

[39] J. A. Oller and U.-G. Meißner, Chiral dynamics in the presence of bound states: Kaon nucleon interactions revisited, Phys. Lett. B **500**, 263 (2001).

[40] L. Roca, E. Oset, and J. Singh, Low lying axial-vector mesons as dynamically generated resonances, Phys. Rev. D **72**, 014002 (2005).

[41] S. Sarkar, B. X. Sun, E. Oset, and M. J. Vicente Vacas, Dynamically generated resonances from the vector octet-baryon decuplet interaction, Eur. Phys. J. A **44**, 431 (2010).

[42] E. Oset and A. Ramos, Dynamically generated resonances from the vector octet-baryon octet interaction, Eur. Phys. J. A **44**, 445 (2010).

[43] B. Borasoy, U.-G. Meißner, and R. Nißler, K- p scattering length from scattering experiments, Phys. Rev. C **74**, 055201 (2006).

[44] Z. W. Liu and S. L. Zhu, Pseudoscalar meson and charmed baryon scattering lengths, Phys. Rev. D **86**, 034009 (2012).

[45] R. Molina, C. W. Xiao, and E. Oset, J/ψ reaction mechanisms and suppression in the nuclear medium, Phys. Rev. C **86**, 014604 (2012).

[46] V. V. Anisovich, M. A. Matveev, J. Nyiri, A. V. Sarantsev, and A. N. Semenova, Non-strange and strange pentaquarks with hidden charm, arXiv:1509.04898.

[47] T. J. Burns, Phenomenology of $P_c(4380)^+$, $P_c(4450)^+$ and related states, arXiv:1509.02460.

[48] Y. J. Zhang, H. C. Chiang, P. N. Shen, and B. S. Zou, Possible S-wave bound-states of two pseudoscalar mesons, Phys. Rev. D **74**, 014013 (2006).

[49] J. Haidenbauer, G. Krein, U. G. Meißner, and A. Sibirtsev, Anti-D N interaction from meson-exchange and quark-gluon dynamics, Eur. Phys. J. A **33**, 107 (2007).

[50] R. Khosravi and M. Janbazi, Vertices of the $D_s^{(*)}D^{(*)}K^*$, arXiv:1509.01715.

[51] B. El-Bennich, G. Krein, L. Chang, C. D. Roberts, and D. J. Wilson, Flavor SU(4) breaking between effective couplings, Phys. Rev. D **85**, 031502 (2012).

[52] K. U. Can, G. Erkol, M. Oka, A. Ozpineci, and T. T. Takahashi, Vector and axial-vector couplings of D and D* mesons in $2+1$ flavor Lattice QCD, Phys. Lett. B **719**, 103 (2013).

[53] Z. H. Li, T. Huang, J. Z. Sun, and Z. H. Dai, Strong couplings of heavy mesons to a light vector meson in QCD, Phys. Rev. D **65**, 076005 (2002).

[54] M. E. Bracco, M. Chiapparini, A. Lozea, F. S. Navarra, and M. Nielsen, D and rho mesons: Who resolves who?, Phys. Lett. B **521**, 1 (2001).

[55] Z. G. Wang, Analysis of the vertices DDV and D^*DV with light-cone QCD sum rules, Eur. Phys. J. C **52**, 553 (2007).

[56] C. Garcia-Recio, J. Nieves, O. Romanets, L. L. Salcedo, and L. Tolos, Hidden charm N and Delta resonances with heavy-quark symmetry, Phys. Rev. D **87**, 074034 (2013).

[57] M. Karliner and J. L. Rosner, New Exotic Meson and Baryon Resonances from Doubly-Heavy Hadronic Molecules, Phys. Rev. Lett. **115**, 122001 (2015).

[58] M. Karliner and J. L. Rosner, Photoproduction of exotic baryon resonances, arXiv:1508.01496.